Civil Engineering Infrastructures Journal xx,xx
DOI: 10.22059/ceij.2025.376471.2059

A Comparative Study of Concrete Material Models for Seismic Analysis of External Beam-to-Column Joints

Mousavizadeh, M.M.[1] and Ghandi, E.[1*]

Department of Civil Engineering, Faculty of Technical and Engineering, University of Mohaghegh Ardabili, Ardabil, Iran

Received: 14/05/2024
Revised: 12/10/2024
Accepted: 30/11/2024

Abstract. In reinforced concrete (RC) moment-resisting frames, beam-to-column joints (BCJs) are essential for the effective transmission of lateral forces, particularly those induced by seismic events. During severe ground motions, these joints are exposed to significant forces, making them a critical zone in RC frames. In order to develop structurally sound and resilient constructions capable of withstanding seismic events, it is imperative to possess an exhaustive comprehension of the behavior of structural joints and the underlying failure mechanisms associated with them. This knowledge forms the foundation for designing robust structural systems that can effectively mitigate the adverse effects of seismic disturbances. This research employed three widely recognized concrete material models available in LS-DYNA software—namely, the Winfrith model, the Concrete Surface Cap Model (CSCM), and the Concrete Damage Plasticity Model (CDPM)—to perform a three-dimensional nonlinear finite element analysis of external BCJs and assess their seismic performance. The simulation outcomes were compared against experimental data to ensure their accuracy and reliability. The findings from the analysis facilitated an

[1] Ph.D. Student, E-mail: moosavizadeh@uma.ac.ir

[1*] Corresponding Author, Associate Professor, E-mail: ghandi@uma.ac.ir

evaluation of the key characteristics of the cyclic behavior of external BCJs, encompassing the hysteresis load-displacement curve, failure modes, stiffness degradation, and pinching effects. Based on these results, the advantages and limitations of each concrete material model are discussed.

Keywords: BCJ, Seismic behavior, Nonlinear FE analysis, Concrete models, LS-DYNA

1. Introduction

The connection between the beam and column is pivotal in determining the seismic performance of reinforced concrete (RC) moment-resisting frames. Design codes stipulate that failure should not occur at the joint prior to the development of a plastic hinge in the beam. Numerous experimental investigations (Lee and Park, 2019; Arowojolu and Ibrahim, 2019; Jin et al., 2018; Unal and Burak, 2013) have demonstrated that failure at the joint may ensue despite plastic hinges in beams. Experimental studies provide a reliable and intuitive method for gaining insights into the actual behavior of structures. However, it is important to acknowledge that they also have notable limitations. Various parameters affect the seismic performance of connections, and it is often not feasible to experimentally investigate all of these facts. Furthermore, conducting large-scale experimental tests requires considerable time and financial resources. In this regard, three-dimensional nonlinear finite element (FE) analysis provides a suitable estimation of the stress and strain distribution in the joint region, progressive damage evolution trend, and force transfer mechanism.

An early exploration of the performance of reinforced concrete beam-column joints (BCJs) utilizing the finite element method was undertaken by Will et al. (1972). They specifically focused on the external corner connection, employing plane stress analysis. Hoehler and Ozbolt (2001) conducted a three-dimensional analysis using the MASA software to assess the behavior of external BCJs during cyclic loading. The model accurately predicted the load-displacement hysteresis curve in most cases, except for those with significant shear deformation. The model successfully captured concrete cracking and strain distribution in the reinforcement, but it is recommended to improve the representation of shear sensitivity by incorporating the Bauschinger effect into the cyclic constitutive model for steel.

Goto and Joh (2004) performed an experimental investigation into the shear strength of four eccentric beam-column connections subjected to cyclic loading. The joints were designed to fail under shear. The predicted results using the DIANA software showed good agreement with the shear failure mechanism in all specimens. However, the ultimate strength was slightly higher than the test results. Ibrahim and El-Badry (2008) conducted a study to analyze the cyclic behavior of external connections. The study assessed the influence of reinforcement detailing on joint behavior. They used ATENA software for numerical analysis. The numerical model showed differences in maximum load and stiffness compared to test results. However, the failure mode was accurately simulated. Sagbas et al. (2011) used Vector2 software to analyze the cyclic behavior of BCJs. They explored the impact of different factors on BCJs, such as the presence of plain and deformed bars, internal and external joints, inadequate confinement, and the use of haunch bars. The numerical modeling aligned closely with the experimental results concerning the load-displacement response, strength, crack pattern, and failure mode. Xing (2019) conducted a numerical investigation on the seismic response of internal BCJs using LS-DYNA software and the concrete model proposed by Moharrami and Koutromanos (2016). The model considers factors like crack opening and closing, concrete strength degradation, and confinement influence. The simulation results matched well with experimental results, especially in specimens with minimal shear cracks. The model effectively captured the pinching effect in specimens without significant shear deformations.

Balamuralikrishnan and Saravanan (2019) conducted an investigation into the behavior of exterior beam-column joints that were internally reinforced with Glass Fibre Reinforcement Polymer (GFRP). This analysis utilized ABAQUS software to evaluate various material properties, loading scenarios, and support conditions. The authors subsequently compared the shear strength of the joints predicted by the simulations with the corresponding experimental results. Tambusay et al. (2020) conducted a nonlinear finite element analysis utilizing ATENA software to simulate three distinct types of joints: an interior joint, an exterior joint, and a corner joint. Each joint type exemplifies typical configurations found in general moment-resisting frame structures. This study evaluates the efficacy of a smeared fixed crack approach in modeling the highly nonlinear behavior of cracked concrete subjected to bidirectional cracking due to reversed cyclic loading. The results demonstrate that the numerical models effectively capture the complete cyclic hysteretic response, along with the progressive degradation of strength and stiffness, the evolution of cracking and damage throughout the loading cycles, and the modes of failure. Bahraq et al. (2021) explored the seismic performance of BCJs constructed with normal concrete and retrofitted with Ultra-High Performance Fiber-Reinforced Concrete (UHPFRC) through both numerical and analytical methodologies. The models were developed in Abaqus, utilizing a concrete damage plastic material to accurately represent both the normal concrete substrate and the UHPFRC overlay. The interaction between these two layers of concrete was modeled using cohesive elements. The results demonstrated that the proposed finite element model closely matched the experimental behavior observed in seismically tested specimens, particularly in terms of global load-displacement characteristics, ultimate load capacity, and damage progression. Moreover, the use of surface-to-surface cohesive elements proved essential for effectively modeling the bonding interface under cyclic loading conditions. Ultimately, the authors aimed to determine the optimal thickness and reinforcement ratios that would enhance the performance of BCJs.

Noor et al. (2024) investigated the effectiveness of steel fiber reinforced concrete (SFRC) within the joint core to enhance ductility and address the construction challenges typically associated with conventional reinforcement techniques. A nonlinear finite element analysis was conducted using ABAQUS software to simulate the behavior of SFRC beam-column joints under cyclic loading conditions. The analysis concentrated on the impact of varying steel fiber volume fractions and aspect ratios on joint performance. The results of this study suggest that the strategic integration of SFRC in the joint core can promote ductile shear failure, improve joint toughness, and alleviate construction complexities by minimizing the need for densely packed hoops. Golias et al. (2024) conducted a three-dimensional finite element analysis using ABAQUS to examine the seismic behavior of reinforced concrete beam-column joints, including those strengthened with carbon fiber reinforced polymer (CFRP) ropes. The CFRP ropes were applied in an X-shape around the joint and as flexural reinforcement on the beam's top and bottom. This configuration aimed to increase principal stresses within the joint core and reduce shear deformation. The study found that the results from the nonlinear analysis concerning the principal stresses in the concrete joint core, force-displacement envelopes and joint shear deformation closely matched experimental data. This alignment confirms that the finite element method accurately represents the behavior of reinforced concrete beam-column connections and highlights the effectiveness of CFRP ropes as a viable strengthening solution.

Shi et al. (2021) carried out a numerical simulation using the OpenSees to assess the cyclic response of steel fiber reinforced concrete (SFRC) beam-column joints. They refined the calculation methods for joint shear and the slip deformations of longitudinal reinforcement. The viability and precision of their numerical modeling approach were confirmed by comparing the computed results with experimental data, with particular emphasis on hysteresis curves, backbone curves, energy dissipation, and stiffness degradation. Zhuang et al. (2024) investigated the seismic behavior of precast beam-column joints with mechanical connections (PBCJs-MCs) using OpenSees. They developed fiber models for PBCJs-MCs grounded in existing experimental data. The numerical results indicate that these fiber models accurately capture the bond-slip relationship between concrete and reinforcement under cyclic loading conditions. The relative errors in the simulated seismic behavior indicators, such as bearing capacity, energy dissipation capacity, and stiffness degradation, are approximately 15%.

Najafi et al. (2024) assessed three experimental reinforced concrete moment frames with different friction dampers—two using transmission mechanism and one utilizing rotation mechanism. They conducted numerical analyses using Abaqus software to evaluate how slip force affected seismic performance. The study emphasized a rotational damper that yielded the best experimental results. Initially, the friction damper was numerically analyzed, leading to an equation for calculating sliding force. Validation of the frame with rotational dampers showed optimal performance when the damper's sliding force was 1.4 times the strength of the bare frame. Ghasemitabar et al. (2020) used LS-DYNA software to validate the seismic performance of external connections with shape memory alloy-based (SMA) bars near the joint panel. The study examined the influence of varying quantities of SMA bars on the seismic response of the connection, including moment-rotation curve, energy dissipation, and failure modes. The Winfrith concrete model defined the behavior of concrete. The validation process showed good accuracy in the lateral load-story drift curve, despite not considering rebar-concrete slippage effects. Mousavizadeh et al. (2024) systematically examined the seismic behavior of four large-scale RC exterior beam-to-column joints through both experimental and numerical methodologies. The objective of this research was to assist the transfer of the plastic hinge in beams through the application of localized weakening techniques. For the numerical analysis, the LS-DYNA software was employed, utilizing the Concrete Damage Plasticity Model (CDPM) for the modeling of concrete. The numerical outcomes are consistent with the experimental observations concerning the load-displacement hysteretic response and the failure mode.

The objective of the current study is to examine the cyclic response of RC external beam-to-column connections utilizing the LS-DYNA software. LS-DYNA is a nonlinear finite element hydro-code specifically designed to analyze structures and fluid-structure coupling with large deformations in static and dynamic scenarios (Hallquist, 2006). In the analysis of reinforced concrete structures, LS-DYNA offers two significant advantages over other finite element software. First, it provides users with greater flexibility in selecting concrete models, owing to its extensive material library. Second, the concrete constitutive models within LS-DYNA are adept at simulating the pinching phenomenon observed in the cyclic behavior of reinforced concrete, even in the absence of considerations for bond-slip between concrete and reinforcing bars. The Table 1 presents a diverse array of concrete models available in LS-DYNA. Among these models, five commonly used ones include the Karagozian and Case (K&C) concrete model Release3, the RHT concrete model, the Winfrith Concrete model, the Concrete Surface Cap Model (CSCM), and the Concrete Damage Plastic Model (CDPM). The K&C model is particularly efficient for analyzing concrete structures that are subjected to impulsive loading (LS-DYNA User's Manual Vol.2, 2018), while the RHT model is suitable for impact and porous compaction analyses (Tu and

Lu, 2010). However, these two models exhibit poor performance under cyclic loading (Gharavi et al., 2022, Asgarpoor et al., 2021, Zhao et al., 2021, Bohara et al. 2019), and therefore, they are not extensively discussed in this particular study. The last three models were formulated based on a combination of plasticity and smeared cracking or plasticity and continuum damage approach. These models were briefly explained and utilized for validation purposes.

2. Concrete material models

2.1. Winfirth Concrete Model

The Winfrith concrete model was first presented by Broadhouse and Neilson and subsequently enhanced by Broadhouse (LS-DYNA User's Manual Vol.2, 2018). The plasticity aspect of this model is founded on the shear failure surface suggested by Ottoson (Schwer, 2011) and is expressed through a four-parameter equation:

Table 1.Various concrete models available in the LS-DYNA material library

Concrete Constitutive Model	LS-DYNA material designation
Mat-Pseoudo -Tensor	Mat016
Mat- Geologic - Cap Model	Mat025
Mat- Concrete -Damage	Mat072
Mat- Soil- Concrete	Mat078
Mat-Winfirith- Concrete	Mat084/085
Mat- Brittle Damage	Mat096
Mat-Johnson- Helmquist-Concrete	Mat111
Mat-Schwer-Murray-Cap Model	Mat145
Mat- Concrete -Surface_Cap Model (CSCM)	Mat159

Mat-Concrete-EC2	Mat172
Mat-RC- Beam	Mat174
Mat-RHT	Mat272
Mat- Concrete Damage Plastic Model	Mat273

$$F(I_1, J_2, cos\theta) = a\frac{J_2}{(f_c')^2} + \lambda\frac{\sqrt{J_2}}{f_c'} + b\frac{I_1}{f_c'} - 1 \quad (1)$$

In Equation (1), the constants a and b regulate the meridional shape of the shear failure surface, while $\lambda = \lambda(cos3\theta)$ dictates the shape of the shear failure surface on the octahedral plane (π -plane) within the limits $0 \leq \theta \leq \frac{\pi}{3}$. The value of λ varies from -1 to +1, which corresponds to triaxial compression and triaxial extension, respectively. The constants a and b are influenced by the ratio of the unconfined tensile strength f'_t to the unconfined compressive strength f'_c, in addition to their direct dependence on f'_c. Here, I_1 represents the first invariant of Cauchy's stress tensor, J_2 is the second invariant of the deviatoric stress tensor, and $\cos 3\theta = \frac{3\sqrt{3}}{2}\frac{J_3}{J_2^{1.5}}$ where J_3 is the third invariant of the deviatoric stress tensor. The angle θ is commonly known as the Lode Angle. For more in-depth studies in this field, Schwer (2011) can be referred to. Furthermore, the Winfrith model allows each element accommodate tensile cracks with up to three orthogonal crack planes. The shear capacity across the crack plane is influenced by the aggregate size, but it does not directly affect the material's softening behavior (Schwer, 2011). The softening behavior under tension can be incorporated into the analysis by specifying the crack width or fracture energy. Apart from the ability to represent the position, orientation, and width of cracks, the Winfrith model can also consider the effects of strain rate.

2.2. Concrete Surface Cap Model (CSCM)

The concrete surface cap model was initially developed to simulate concrete failure resulting from vehicle impact on roadside safety structures. As shown in Figure 1, this model aims to represent the yield behavior of concrete under complex stress states through the continuous intersection of two components including the shear yield surface and the hardening cap. The yield surface is defined as a function of three stress invariants: the first

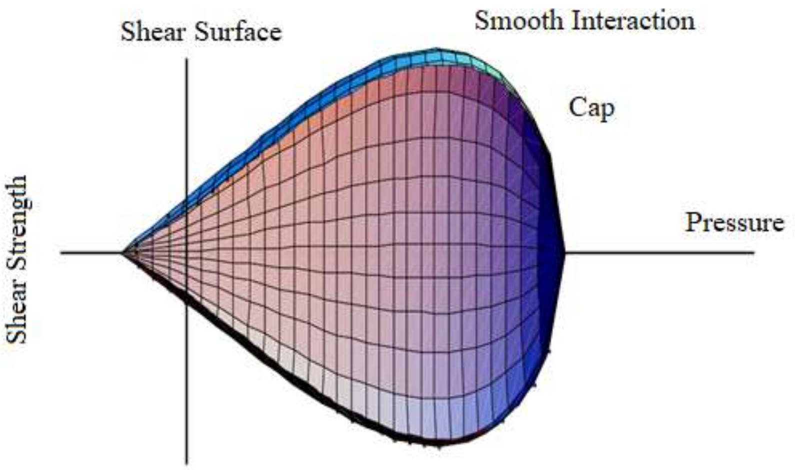

Figure 1. The general shape of concrete model yield surface (LS-Dyna User's Manual, Vol2, 2018)

invariant of the stress tensor, along with the second and third deviatoric stress invariants. To account for plastic volumetric changes due to pore collapse, a surface cap is employed, despite the fact that individual pores are not explicitly represented in this framework. The shear surface characterizes the strength of concrete under tensile conditions and low confining pressures, whereas the interaction between the cap and shear surfaces effectively represents its strength across a spectrum from low to high confining pressures. (LS-DYNA User's Manual Vol.2, 2018). The surface cap model for concrete considers the strain-softening behavior under tension and the reduction in the modulus of concrete through an isotropic damage formulation (Jiang and Zhao, 2015). The model incorporates the effects of strain rate through viscoplasticity (LS-DYNA User's Manual Vol.2, 2018).

2.3. Concrete Damage Plastic Model (CDPM)

The CDPM is a plasticity model that integrates specific damage mechanisms associated with concrete and was developed by Grassl and Jirasek (2006). This model captures the fundamental characteristics of the failure mechanisms of concrete when subjected to multi-axial and rate-dependent loading conditions. It integrates a plasticity framework grounded in effective stress with a damage model that utilizes both plastic and elastic strain measures. The plasticity component of the model is defined within the effective stress space utilizing Haigh-Westergard stress coordinates, which consist of the volumetric effective stress, the norm of the deviatoric effective stress, and the Lode angle. (LS-DYNA User's Manual Vol.2, 2018). The yield surface is determined through the extension of the failure envelope. This failure envelope is characterized by curved meridians and deviated sections, whose geometry varies from triangular to almost circular depending on the loading conditions under tension and high confining compresion, respectively. (Grassl et al., 2018). Damage is primarily characterized in both tensile and compressive states, enabling a more accurate depiction of cracking and crushing behavior.

Figure 2 shows three methods - linear, bilinear, and exponential - for defining tensile damage based on stress-inelastic displacement law, where f'_t, $\varepsilon_{t,}$ and w_f are uniaxial tensile strength, inelastic tensile strain, and displacement, respectively. The variable h is a mesh-dependent parameter used to convert strains to displacements. As shown in Figure 3, the compressive damage is controlled by an exponential relationship for stress-inelastic strain, using the uniaxial compressive strength of concrete f'_c and inelastic strain ε_{fc}. The default value of the inelastic strain parameter is 0.0001, and smaller values of this strain indicate a relatively brittle state of damage (LS-DYNA User's Manual Vol.2, 2018). To mitigate the risk of premature failure in areas adjacent to supports or applied loads, and to enhance the ductility of the compression response, it is essential to select a value for this parameter that exceeds its default setting.

A review of past research shows that although the material library of LS-DYNA provides various models for concrete modeling, it is less commonly used compared to other available finite element software to simulate the seismic behavior of reinforced concrete structures.

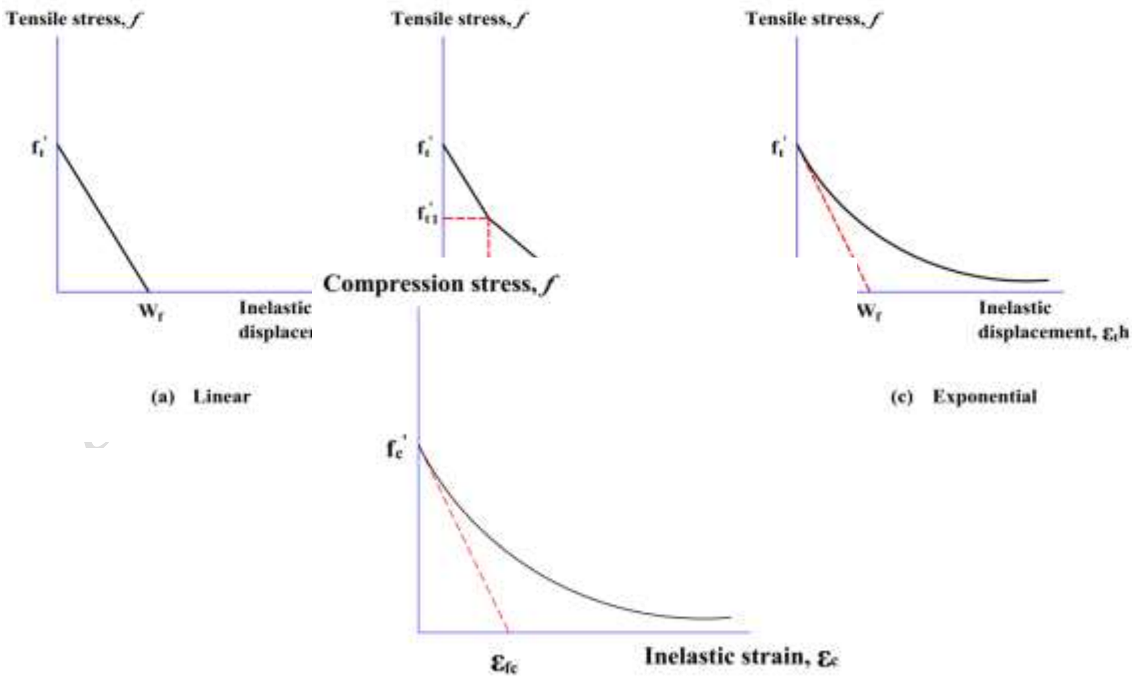

Figure 3. Compressive damage law in CDPM

3. Experimental database

In this research, the CBCJ specimen, which was previously tested by Rezvanisharif and Ketabi (2020), was selected for validation in LS-DYNA using three concrete models - Winfrith (Mat84), Concrete Surface Cap model (CSCM-Mat159), and Concrete Plastic Damage Model (CDPM-Mat273)—the experimental study aimed to use X-form reinforcement details for plastic hinge relocation away from the joint region. The specimen was designed and fabricated based on the requirements for special moment frames in the ACI 2014 Standard. It was subjected to cyclic loading up to a drift ratio of 8% to simulate severe earthquakes. The geometry, reinforcement details of the specimen, and loading protocol are shown in Figure 4. The experimental test was conducted under quasi-static conditions with reversed lateral cyclic loading under displacement control mode. At each drift ratio, three complete cycles were applied to the end of the beam. A constant axial load equal to 11% of the axial capacity of the column was applied to the end of the column throughout the duration of the test. The clear concrete cover on the outer edge of the stirrups is 20 mm. The mechanical properties of the concrete at the time of testing, along with those of the reinforcing bars, are presented in Table 2.

4. Numerical analysis of specimen CBCJ

This section provides the results of simulating the CBCJ specimen under cyclic loading using three concrete material models in LS-DYNA. The study validated and investigated the seismic response of the specimen, including the load-displacement hysteretic curve and the failure mode of the joint.

4.1. The type of elements

The concrete elements were modeled using 8-node hexahedron solid elements with reduced integration formulation, which significantly reduces analysis time. However, the main drawback of this method is the need to control the hourglass modes, which can cause abnormal deformations in elements. Therefore, controlling hourglass modes for solid elements with reduced integration has always been recommended (Hallquist, 2006). An example of abnormal deformations caused by hourglass modes is shown in Figure 5. The steel reinforcements were simulated using a piecewise linear plasticity model, which characterizes elastic-plastic behavior while accounting for strain rate effects. The reinforcing bars were modeled as one-dimensional beam elements, utilizing the Hughes-Liu formulation for two-node beam elements.

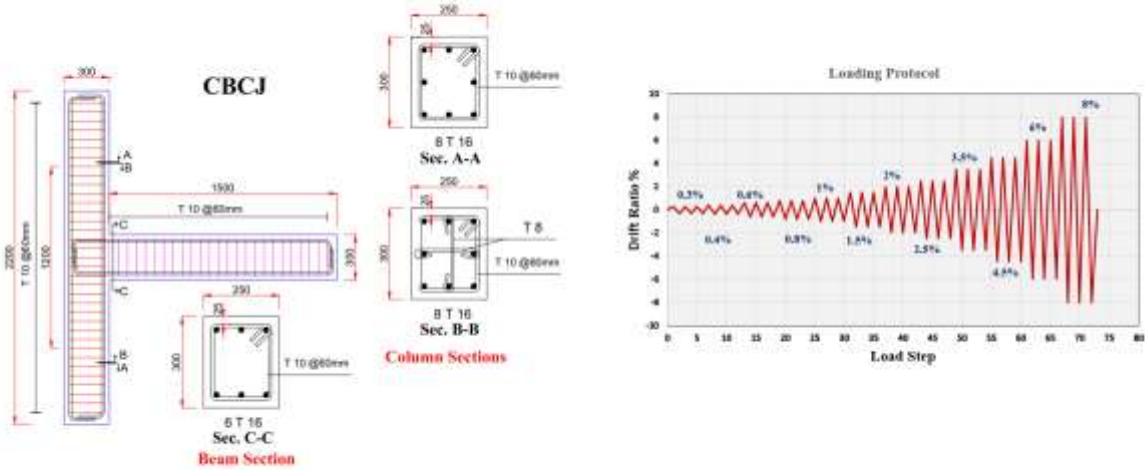

Figure 4. Geometry, Reinforcement Details, and Loading Protocol (Rezvanisharif and Ketabi, 2020)

Table2. Mechanical Properties of Materials (Rezvanisharif and Ketabi, 2020)

Concrete		Steel Rebars			
		Diameter (mm)	8	10	16
Cylinder compressive strength (f_c') - MPa	51.4	Young's modulus (GPa)	198.5	195.2	197.1

Prism tensile strength (f_t) -MPa	2.5	Yield stress (MPa)	428.1	427.4	425.2
Elasticity modulus - GPa	33.7	Ultimate stress (MPa)	664	664.5	651.2

This formulation is consistent with brick elements, as it is based on the degenerated brick element formulation (LS-DYNA User's Manual Vol.2, 2018). To incorporate the reinforcing steel bars within the concrete in LS-DYNA, two general methods are commonly employed: smeared reinforcement and explicit reinforcement. In the smeared reinforcement method, it is assumed that the reinforcing bars are distributed uniformly inside the concrete element along a specific direction. This approach utilizes the average volumetric ratio of the material properties to homogenize the composite properties of concrete and steel (Schwer, 2014).

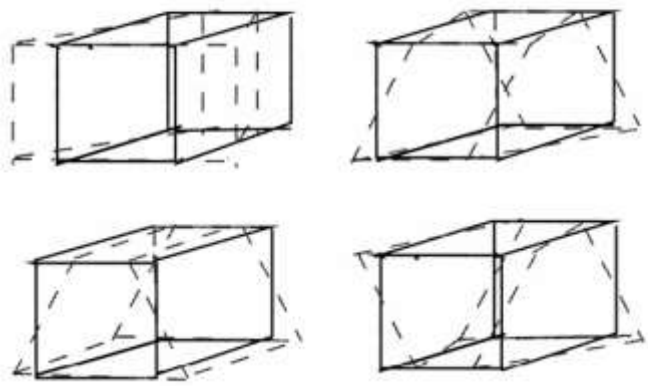

Figure 5. The hourglass modes of an 8-node solid element with one integration point. A total of 12 modes exist (LS-DYNA User's Manual Vol.2, 2018)

The smeared reinforcement method is suitable for analyses where deformations are small, and the behavior of the reinforcing bars remains in the elastic range. Two approaches, the shared (merged) node method, and the constrained method, are utilized to explicitly account for the influence of reinforcing bars within the concrete in structural analysis. The shared node method necessitates the concrete and bar elements to share identical nodes. In this method, the bond between concrete and reinforcing bars can be simulated by employing a perfect bond or incorporating linkage elements to consider the bond-slip relationship. However, employing the shared node meshing method can be complex when dealing with three-dimensional layers of reinforcing bars, such as longitudinal bars and stirrups. In this research, the constrained method was employed to incorporate the reinforcing bars within the concrete. Separate meshes for the concrete and reinforcing bars were constructed and subsequently integrated in a manner ensuring compatibility of their degrees of freedom in specific directions. The interaction between the concrete and reinforcing bars was modeled assuming a perfect bond, without accounting for the effects of slippage.

4.2. mesh-size effect

The mesh size is determined by the size and shape of the specimen, but a very fine mesh will result in long computation times, while an excessively coarse mesh will negatively impact the accuracy of the prediction. The impact of mesh size on the cyclic behavior of joint is assessed using CDPM model. To design purposes, it is necessary to determine the load corresponding to the failure mode. As a result, the measured ultimate strength of the specimen was designated as a criterion for evaluating the model's accuracy, so that the appropriate mesh dimensions could be selected. For this purpose, four finite element models with different mesh dimensions were analyzed as described in Table 3.

Table 3. mesh data for the simulated models

name	mesh size (mm)	concrete elements
model 1	25x25x25 (whole model)	17760
model 2	50x50x50 (whole model)	2220
model 3	25x30x30 (whole model)	12400
model 4	25x30x30 (critical regions) 25x30x50 (remaining parts)	10200

Figure 6a compares the load-displacement hysteresis curve of models 1 and 2 with the test result. The model with the coarse mesh has a 20% error (average error of ultimate strength in the positive and negative load direction) compared to the test, while the model with the fine mesh has a 10% error. Models 3 and 4 were evaluated with the aim of minimizing computational costs while ensuring that the accuracy of the results remained within acceptable ranges. In the model 3, a uniform mesh with dimensions of 25 x 30 x 30 mm was employed for the concrete elements. In Model 4, a mesh size of 25 x 30 x 30 mm was utilized in critical regions, such as the joint panel, around the support points, and in regions adjacent to the applied lateral load. In contrast, a mesh size of 25 x 30 x 50 mm was used in the remaining parts of the model. Figure 6b presents the load-displacement hysteresis curve of models 3 and 4. The model 3 with the uniform mesh has a 10.5% error compared to the test, while the model 4 with the hybrid mesh has a 11% error. Model 4 exhibited the shortest analysis time compared to the other models while maintaining a good accuracy in its results. Consequently, the findings from the analysis of this model are presented in the following sections.

It should be noted that to mitigate the impact of the aspect ratio on the analysis results, a maximum aspect ratio of 1.2 was established for the critical areas of the model 4. This selected ratio is below the recommended maximum value of 1.5 (Rezavanisharif and Ketabi, 2019; Zhao et al., 2021). The longitudinal reinforcing bars were also meshed based on their location relative to the concrete elements, which had dimensions of 30 and 50 mm. The model 4 consisted of 13,402 elements, including 2,842 beam elements and 10,200 solid elements. Figure 7 illustrates the finite element model developed for Model 4.

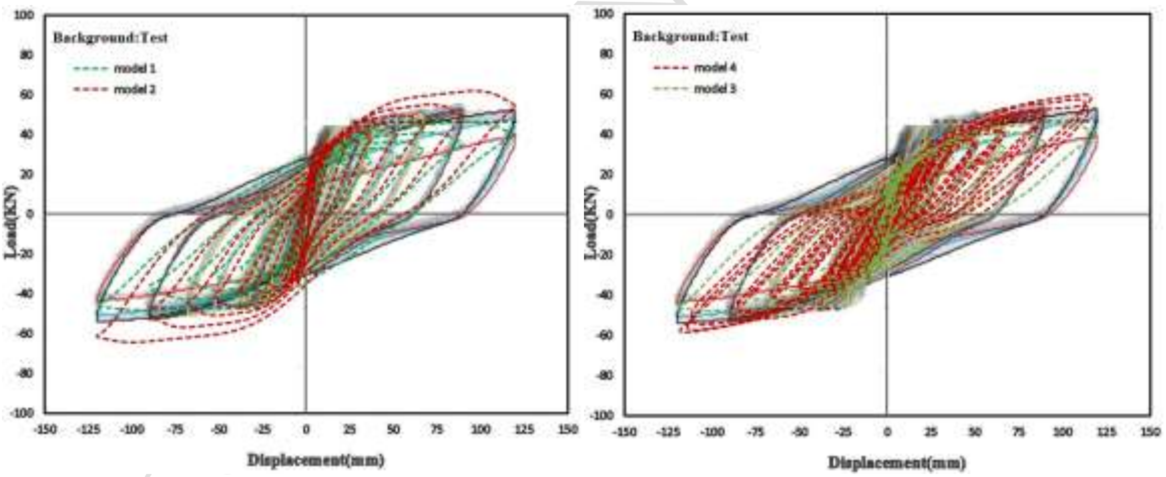

(a) (b)

Figure 6. effect of mesh size on load-displacement diagram of model

Considering the quasi-static loading conditions of the laboratory test, the implicit method was deemed suitable for numerical analysis. However, due to the highly nonlinear behavior of concrete observed in the experimental test and to prevent numerical divergence, the explicit method was utilized in this study. Consistent with the experimental test conditions, roller and hinge supports were incorporated into the model.

5. FE results and discussion

5.1. Hysteresis load-displacement curves

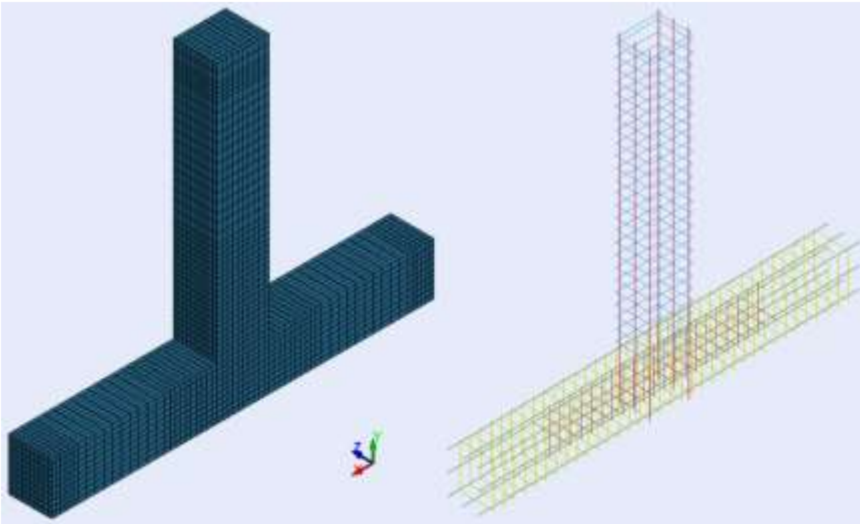

Figure 8 illustrates the load-displacement hysteretic curves obtained from simulations using three different concrete materials, compared with the test result. These curves are plotted based on the horizontal displacement applied at the end of the beam and the corresponding load. The experimental test results indicate that the specimen exhibited ductile behavior, with no substantial reduction in strength observed. Additionally, the specimen experienced some degree of pinching. Table 4 reports the key parameters of the hysteretic curves, including yielding strength, ultimate strength, initial stiffness, displacement ductility, and energy dissipation capacity.

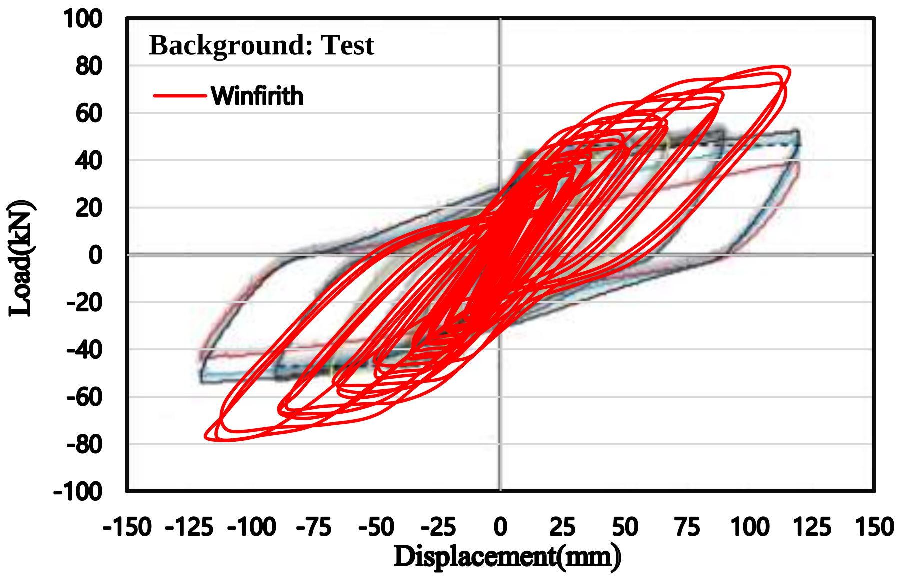

Based on the analysis results, the CDPM model exhibited higher accuracy in predicting the cyclic behavior of the RC external beam-to-column connection compared to the other two concrete material models. It successfully captured phenomena such as pinching, strength degradation, and stiffness degradation. In contrast, the CSCM model failed to detect pinching and stiffness degradation, showing a continuous increase in load capacity. The Winfrith model, utilizing a smeared crack formulation that considers the opening and closing of cracks, demonstrated relatively accurate predictions for the yield strength, with an average error of 6.13% (averaged between the push and pull directions). However, the average error for the ultimate strength was higher at 38.2%. Nevertheless, the Winfrith model was able to simulate pinching effects, even without considering the bond-slip relationship. As a result, it provided a better estimation of energy dissipation. Despite the absence of information regarding the maximum aggregate size in the experimental study, it is important to emphasize that adjusting the maximum aggregate size from 10 millimeters to 12 and 14 millimeters did not yield a notable impact on the resulting hysteretic curve within the model.

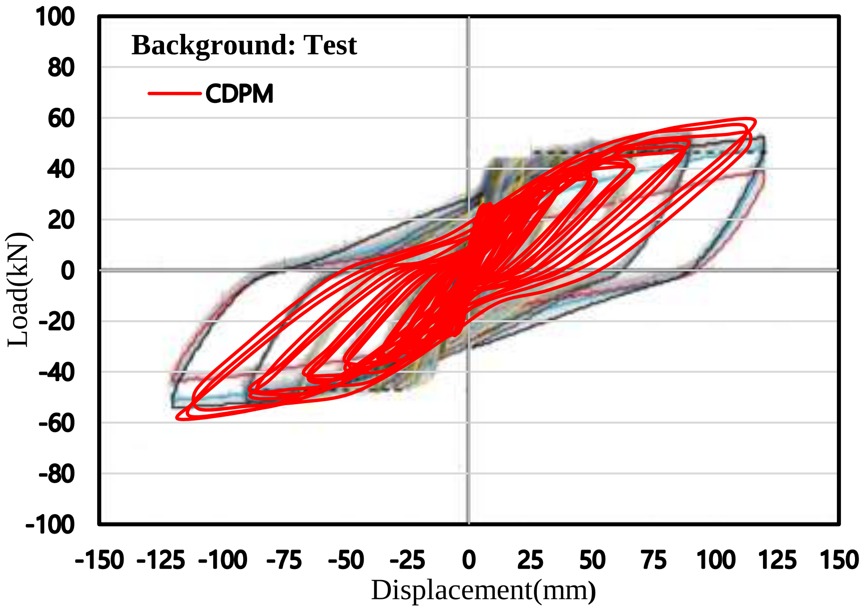

Figure 8. **Load-Displacement Hysteresis Curve, Comparison between Models and Test**

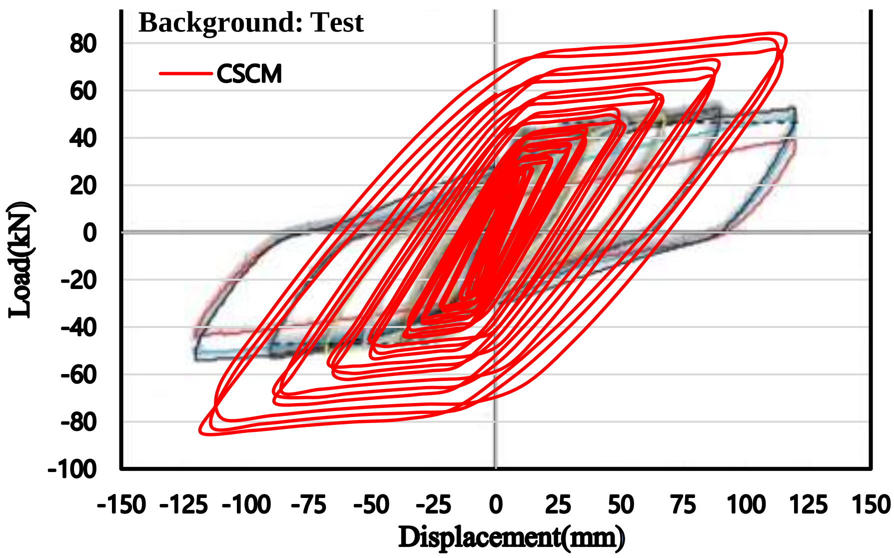

Figure 8. **Continued**

The CDPM model demonstrated accurate predictions for both the yield strength and the ultimate strength, with average errors of 6.32% and 11%, respectively. Consequently, it provided the best estimations for the load-carrying capacity at various loading stages. This model integrates both damage and plasticity, enabling effective simulation of concrete's nonlinear behavior under cyclic loading. Its parameters are calibrated using experimental data from cyclic tests, enhancing predictive capabilities across various loading conditions. The model accurately represents hardening and softening behavior during repeated loading, improving predictions of cyclic behavior. Additionally, CDPM can manage complex stress states, essential for accurately simulating beam-to-column connections under seismic loads. It also accounts for damage accumulation and material property degradation over cycles, which is critical for realistic seismic event simulations.

The CDPM model effectively simulated pinching effects, even exhibiting more pronounced pinching in the later cycles of loading compared to the test. However, this led to a higher error in the estimation of energy dissipation capacity than the Winfrith model. The reason for the increased pinching in the CDPM model can be attributed to the method employed for calculating the mesh-dependent parameter "h" in LS-DYNA. This parameter is utilized to convert strains into displacements. The tensile fracture energy of concrete, denoted as G_f is defined as the area under the stress-inelastic displacement curve. For the bilinear curve (Fig.2b), this results in $G_f = (f_t' W_{f1} + f'_{t1} W_f)/2$. By using default values of, $f'_{t1} = 0.3 f'_t$ and $W_{f1} = 0.15 W_f$ in CDPM, it follows that $G_f = 0.225 f'_t W_f$. Consequently, the tensile threshold value, which refers to the crack opening threshold or inelastic displacement, is associated with the area under the stress-crack opening curve (fracture energy) as $W_f = 4.444 \frac{G_f}{f'_t}$. However, users cannot directly input this parameter for finite analysis in LS-DYNA. In LS-DYNA, the inelastic strain is calculated as $\varepsilon_t = \frac{W_t}{h}$, where "h" is a measure of the element length, calculated as a function of the element's volume ($h = \sqrt[3]{V_e}$). This method of estimating element length tends to overestimating the fracture energy and, consequently, the crack opening threshold in the simulation.

5.2. Damage and cracking pattern of CBCJ

Figure 9 compares the damage pattern in the CBCJ specimen between the models and the test result at an 8% drift ratio. The maximum principal strain contour has been selected as the criterion for indicating damage in the models, as cracking is the predominant failure mode observed in the tests. Given that the strain ranges across various material models differ, the contour range has also been shown. The CBCJ specimen demonstrated ductile behavior during the test and satisfied the expectations outlined in the design code (ACI2014). This indicates that a plastic hinge was formed in the beam, and the majority of cracks observed in the beam were flexural cracks. Figure 9 illustrates that, in the Winfrith model, significant damage occurred inside the joint panel, which differs from the actual test results. On the other hand, both the CSCM and CDPM models effectively predicted the location and pattern of damage.

The Winfrith model internally generates certain parameters based on undocumented data fittings, particularly the ratio of unconfined tensile to compressive strengths. This lack of user-defined flexibility may lead to inaccuracies if the generated parameters do not accurately represent the material behavior under specific conditions. Furthermore, the model's approach to crack development—where cracks may "heal" during loading cycles—can result in discrepancies in predicting failure modes, particularly in cyclic loading scenarios. Additionally, in the Winfrith model, by setting the RATE parameter to 1 or 2, the effects of strain rate are disregarded. Consequently, the value input by the user for the FE parameter will correspond to the width of the crack. In this context of tensile cracking, the strain softening response is simplified to a linear representation. Users can calculate the crack width (w) at zero stress using the equation $w = 2\frac{G_f}{f_t}$, where G_f represents the specific fracture energy and f_t denotes the concrete tensile strength. In the absence of suitable laboratory data, relying on mathematical relationships to determine the fracture energy may lead to inaccuracies in predicting failure modes.

Table 4. Key Parameters of CBCJ Hysteresis Curve

push direction is positive		**Test**	**Mat84**	**Mat159**	**Mat273**	**Error(%)**		
pull direction is negative						**Mat84**	**Mat159**	**Mat273**
Yielding Strength	**δ_y(mm)**	14.8	14.50	14.73	14.51	-2.05	-0.45	-1.97
		-12	-14.29	-14.28	-14.27	19.07	18.96	18.90
	P_y(kN)	46.5	43.20	38.60	43.67	-7.10	-16.99	-6.09
		-45.5	-43.15	-39.97	-42.52	-5.16	-12.15	-6.55
Ultimate Strength	**δ_u(mm)**	120	120	120	120	0.00	0.00	0.00
		-120	-120	-120	-120	0.00	0.00	0.00

	P_u(kN)	53.5	72.03	76.77	58.98	34.64	43.50	10.20
		-52.3	-74.19	-78.85	-58.48	41.85	50.76	11.82
Initial Effective Stiffness	K_e (kN/mm)	3.1	2.98	2.62	3.01	-3.87	-15.48	-2.90
		3.8	3.02	2.80	2.98	-20.53	-26.32	-21.58
Displacement Ductility	$\mu = \frac{\delta_u}{\delta_y}$	8.1	8.28	8.15	8.27	2.19	0.56	2.11
		10	8.40	8.41	8.41	-16.01	-15.94	-15.90
Energy Dissipation	**E(kN.m)**	89.7	80.23	137.12	52.3	-10.56	52.87	-41.69

In the test, concrete crushing occurred. The simulation of concrete crushing may be accomplished by excluding concrete elements from the analysis. Both the CSCM and CDPM models can automatically consider concrete damage. In the Winfrith plasticity model, which employs a smeared cracking approach, the automatic calculation of concrete damage under

Test

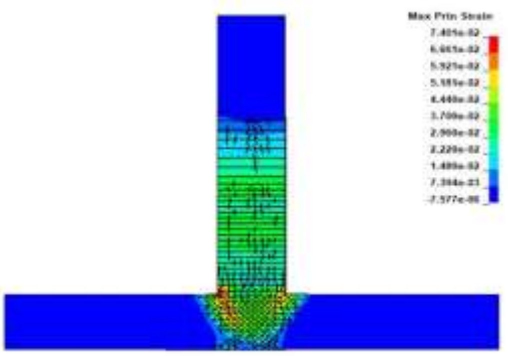

Winfirith

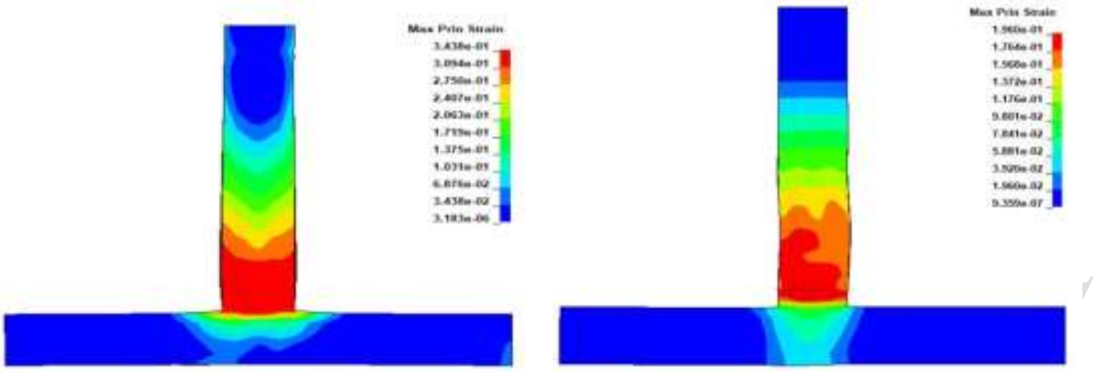

CSCM CDMP

Figure 9. Comparison of damage pattern between test (Rezvanisharif and Ketabi, 2020) and models

compression is not supported. To account for concrete damage, the user is required to define the erosion strain in the software. This can be achieved using the MAT-ADD-EROSION keyword in LS-DYNA, where a suitable value for the minimum principal strain is specified as the criterion for concrete element failure. The failure strain is influenced by factors such as the concrete grade, confinement, loading rate, and stress state. The inherent variability of concrete properties, coupled with its complex nonlinear behavior—particularly under cyclic loading—complicates the determination of a singular erosion strain value. This challenge is further exacerbated by the limited experimental data available on erosion strain for various types of concrete and under differing loading conditions. However, determining an appropriate erosion strain value remains a challenge in the literature. In this particular study, concrete element erosion was considered within the CSCM model as an example. However, it did not significantly impact the hysteretic behavior observed in the load-displacement curve. The ultimate state of joint damage, taking into account the element erosion, is displayed in Figure 10.

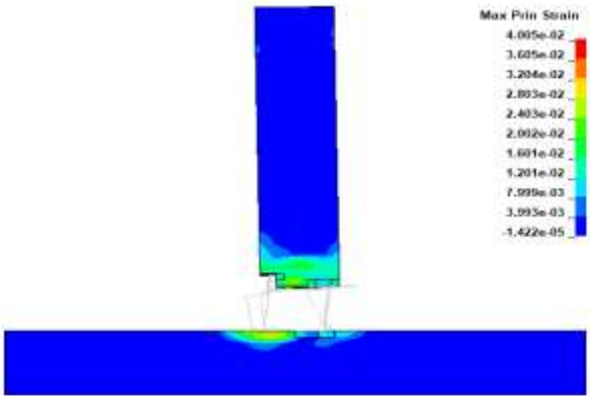

Figure 10. Damage pattern in the CSCM model considering elements erosion

5.3. Stiffness Degradation

In Figure 11, the secant stiffness of the CBCJ models is compared with the test result for the first cycle of each drift ratio. The secant stiffness represents the slope of a straight line drawn between peak-to-peak points of the hysteretic loop. For drift ratios up to 1%, all three models show almost the same cyclic stiffness that deteriorates faster than the test. For drift ratios between 1% to 6%, the CDPM model exhibits the highest rate of stiffness degradation compared to the other two models. After this drift level, it closely matches the stiffness obtained from the test. The CDPM model effectively captures crack initiation and propagation, leading to notable stiffness reduction as the drift ratio increases. The model accounts for the nonlinear behavior of concrete under cyclic loading. As the material yields, the stiffness decreases more rapidly due to the plastic deformation. This model is designed to simulate the accumulation of damage over cycles. As the drift ratio increases, the damage accumulates more quickly, resulting in higher rates of stiffness degradation. The cyclic stiffness predicted by the Winfirith and CSCM models is relatively identical.

5.4. Energy Dissipation

Figure 12 demonstrates the dissipated energy resulting from the developing of plastic hinges in the beam longitudinal bars, and the opening and closing of concrete cracks. The total cumulative energy dissipation at each drift ratio is determined by calculating the sum of the areas enclosed by the hysteretic loops up to that specific drift ratio. According to the figure, the Winfrith material model offers the closest approximation of the total energy dissipation capacity compared to the other two models. The CSCM model overestimates the energy dissipation capacity, while the CDPM model underestimates it.

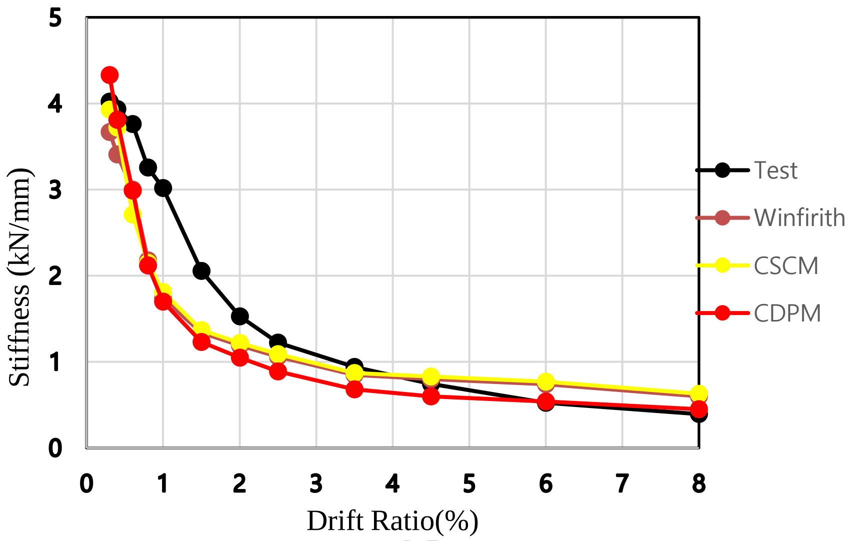

Figure 11. Degradation of secant stiffness

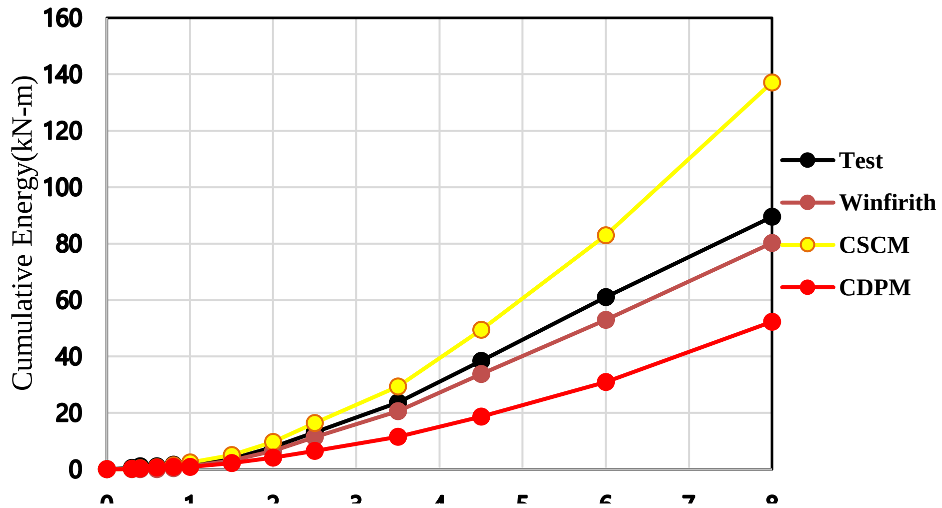

Figure 12. Cumulative energy dissipation capacity

6. Summary and Conclusion

This paper provides a comprehensive review of previous research on the seismic behavior of reinforced concrete beam-to-column connections using three-dimensional nonlinear finite element analysis. Most of the studies in this field did not utilize the LS-DYNA software, which offers various material models for concrete, each with its advantages and limitations. To fill this research gap, three commonly used material models in LS-DYNA, namely Winfrith, CSCM, and CDPM, were selected to validate and investigate the cyclic behavior of external RC beam-to-column connections. The study evaluated several aspects of the connection's cyclic response, including hysteretic behavior, failure mode, yielding and ultimate strength, displacement ductility, energy dissipation capacity, and stiffness degradation. The findings of this research are as follows:

1- The CSCM model demonstrates a continuous increase in maximum load across cyclic loading cycles, which contradicts the expected decrease in stiffness and strength due to material damage accumulation. Therefore, this model lacks accuracy in predicting the seismic hysteresis curve of the joint. The Winfrith model demonstrates certain limitations when it comes to accurately estimating the ultimate load capacity of the connection. However, it effectively captures pinching effects without considering the rebar’s bond-slip relationship in the model. The CDPM model provides the most accurate predictions for the ultimate strength, with average difference of 11%. Although it overestimates crack width in its constitutive relationships, this model offers sufficient accuracy in evaluating the overall seismic performance of the RC external joint.

2- The Winfrith model incorrectly identifies the location of damage within the joint region, while the CSCM and CDPM models accurately predict the location and pattern of damage, even without considering concrete erosion. Precisely simulating the location and pattern of failure has always been a challenge in numerical modeling.

3- Both the CSCM and CDPM models achieve an initial stiffness with an error rate below 5% in the push direction and approximately 21% in the pull direction, indicating acceptable performance.

4- The Winfrith model underestimates the energy dissipation capacity by approximately 11% compared to test results, displaying the best prediction performance in this aspect. Conversely, the CDPM model has an error rate of approximately 41%. When employing the CDPM model, there is an increased occurrence of pinching effects in the hysteresis curve. As a consequence, this leads to a decrease in the energy dissipation capacity and an increase in the error rate of the CDPM model.

References

Arowojolu, O. and Ibrahim, A. (2019). "Plastic hinge relocation in exterior reinforced beam–column joint and compliance issues to seismic design guidelines—A review", Structural Concrete, 21(5), 1938–1958. https://doi.org/10.1002/suco.201900008.

Asgarpoor, M., Gharavi, A. and Epackachi, S. (2021). "Investigation of various concrete materials to simulate seismic response of RC structures", Structures, 29, 1322–1351. https://doi.org/10.1016/j.istruc.2020.11.042.

Bahraq, A.A., Al-Osta, M.A., Khan, M.I. and Ahmad, S. (2021) "Numerical and analytical modeling of seismic behavior of beam-column joints retrofitted with ultra-high performance fiber reinforced concrete", Structures, 32, pp. 1986-2003. https://doi.org/10.1016/j.istruc.2021.04.004.

Balamuralikrishnan, R. and Saravanan, J. (2019) "Finite element analysis of beam-column joints reinforced with GFRP reinforcements", Civil Engineering Journal, 5(12), pp. 2708-2726. https:// 10.28991/cej-2019-03091443.

Bohara, R. P., Tanapornraweekit, G. and Tangtermsirikul, S. (2019). "Investigation of concrete material models for analysis of seismic behavior of reinforced concrete under reversed cyclic load", Songklanakarin Journal of Science and Technology (SJST), 41(4), 951–958. https://doi.org/10.14456/sjst-psu.2019.120.

Gharavi, A., Asgarpoor, M. and Epackachi, S. (2022). "Evaluation of plasticity-based concrete constitutive models under monotonic and cyclic loadings", Structural Design of Tall and Special Buildings, 31(6). https://doi.org/10.1002/tal.1919.

Ghasemitabar, A., Rahmdel, J. M. and Shafei, E. (2020). "Cyclic performance of RC beam-column joints enhanced with superelastic SMA rebars", Computers and Concrete, 25(4), 293–302. https://doi.org/10.12989/cac.2020.25.4.293.

Golias, E., Touratzidis, P. and Karayannis, C.G. (2024) "Seismic response of RC beam-column joints strengthened with FRP ropes, using 3D finite element: verification with real scale tests", CivilEng, 5(2), pp. 395-419. https://doi.org/ 10.3390/civileng5020020.

Goto, Y. and Joh, O. (2004). "Shear resistance of RC interior eccentric beam-column joints", *In Proceedings of the 13th World Conference on Earthquake Engineering (13WCEE)*, Vancouver.

Grassl, P. and Jirásek, M. (2006). Damage-plastic model for concrete failure. International journal of solids and structures, 43(22-23), 7166-7196. https://doi.org/10.1016/j.ijsolstr.2006.06.032.

Grassl, P., Johansson, M. and Leppänen, J. (2018). "On the numerical modelling of bond for the failure analysis of reinforced concrete", Engineering Fracture Mechanics, 189, 13–26. https://doi.org/10.1016/j.engstruct.2020.111612.

Hallquist, J. O. (2006). "LS-DYNA theory manual", Livermore Software Technology Corporation.

Hoehler, M. S. and Ozbolt, J. (2001). "Three-dimensional reversed-cyclic analysis of reinforced concrete members using the microplane", *Otto-Graf Journal*, 12, 93.

Ibrahim, H. and El-Badry, M. (2008). "Nonlinear 3D finite element analysis of exterior beam-column joints reinforced with double studs for shear resistance under cyclic loading", *In Proceedings of the Annual Conference*, Montreal.

Jiang, H. and Zhao, J. (2015). "Calibration of the continuous surface cap model for concrete", Finite Elements in Analysis and Design, 97, 1–19. https://doi.org/10.1016/j.finel.2014.12.002.

Jin, L., Miao, L., Han, J., Du, X., Wei, N. and Li, D. (2018). "Size effect tests on shear failure of interior RC beam-to-column joints under monotonic and cyclic loadings", Engineering Structures, 175, 591–604. https://doi.org/10.1016/j.engstruct.2018.08.092.

Lee, J. Y. and Park, J. (2019). "Effect of strain penetration on RC beam–column joints subjected to seismic loading", In Concrete Structures in Earthquake (pp.309-327). Springer, Singapore. https://doi.org/10.1007/978-981-13-3278-4_18.

L. S. T. C. (2018). "LS-DYNA keyword user's manual volume II material models", Livermore, CA: L. S. T. C.

Moharrami, M. and Koutromanos, I. (2016). “Triaxial constitutive model for concrete under cyclic loading”, Journal of Structural Engineering-ASCE, 142(7). https://doi.org/10.1061/(asce)st.1943-541x.0001491.

Mousavizadeh, M.M., Ghandi, E., Farzam, M. and Gholizad, A. (2024). “An experimental and numerical study of plastic hinge relocation in the exterior RC beam-to-column joints with the implementation of the local weakening method”, Engineering Structures, 317, p.118696. https://doi.org/10.1016/j.engstruct.2024.118696

Najafi, S., Aghayari, R., Cheraghi, K. and TahamouliRoudsari, M. (2024). “Experimental and numerical study of the effect of friction damper on the seismic behavior of concrete frame”. Civil Engineering Infrastructures Journal. https://doi.org/ 10.22059/ceij.2024.378792.2088.

Noor, U.A., Jadoon, M.A., Onyelowe, K., Shahzad, A., Ghaedi, K., Alabduljabbar, H. and Javed, M.F. (2024) “Non-linear finite element analysis of SFRC beam-column joints under cyclic loading: enhancing ductility and structural integrity”, Scientific Reports, 14(1), p. 18152. https://doi.org/10.1038/s41598-024-69270-1.

Rezvanisharif, M. and Ketabi, M. S. (2019). “FE modeling and seismic performance evaluation of hybrid SMA-steel RC beam-column joints”, Latin American Journal of Solids and Structures, 16(5) e192. http://dx.doi.org/10.1590/1679-78255272.

Rezvanisharif, M. and Ketabi, M. S. (2020). “An improved plastic hinge relocation technique for RC beam–column joints: experimental and numerical investigations”, Bulletin of Earthquake Engineering, 18, 4191-4225. https://doi.org/10.1007/s10518-020-00855-7.

Sagbas, G., Vecchio, F. J. and Christopoulos, C. (2011). “Computational modeling of the seismic performance of beam-column subassemblies”, Journal of Earthquake Engineering, 15(4), 640–663. https://doi.org/10.1080/13632469.2010.508963.

Schwer, L. (2011). “The Winfrith Concrete Model: Beauty or Beast? Insights into the Winfrith Concrete Model”, *8th European LS-DYNA Users Conference,* Strasbourg.

Schwer, L. (2014). “Modeling rebar: The forgotten sister in reinforced concrete modeling”, *In 13th International LS-DYNA® Users Conference*, Detroit.

Shi, K., Zhu, J., Li, P., Zhang, M., Xue, R. and Zhang, T. (2021) “Numerical simulation on seismic behavior of steel fiber reinforced concrete beam—column joints”, Materials, 14(17), p. 4883. https://doi.org/10.3390/ma14174883.

Tambusay, A., Suryanto, B. and Suprobo, P. (2020) “Nonlinear finite element analysis of reinforced concrete beam-column joints under reversed cyclic loading”, in IOP Conference Series: Materials Science and Engineering, 930(1), p. 012055. IOP Publishing.

Tu, Z. and Lu, Y. (2010). “Modifications of RHT material model for improved numerical simulation of dynamic response of concrete”, International Journal of Impact Engineering, 37(10), 1072–1082. https://doi.org/10.1016/j.ijimpeng.2010.04.004.

Unal, M. and Burak, B. (2013). “Development and analytical verification of an inelastic reinforced concrete joint model”, Engineering Structures, 52, 284–294. https://doi.org/10.1016/j.engstruct.2013.02.032.

Will, G. T., Uzumeri, S. M. and Sinha, S. K. (1972). “Application of finite element method to analysis of reinforced concrete beam-column joints”, *In Proceeding of Specialty Conference on Finite Element Method in Civil Engineering*, CSCE, EIC, Quebec.

Xing, C. (2019). “An Analytical Study on the Behavior of Reinforced Concrete Interior Beam-Column Joints”. Ph.D. Dissertation, Virginia Polytechnic Institute and State University.

Zhao, M., Lehman, D. E. and Roeder, C. W. (2021). “Modeling recommendations for RC and CFST sections in LS-DYNA including bond slip”, Engineering Structures, 229, 111612. https://doi.org/10.1016/j.engstruct.2020.111612.

Zhuang, M.L., Sun, C., Yang, Z., An, R., Bai, L., Han, Y. and Bao, G. (2024) “Numerical investigation on the seismic behavior of novel precast beam–column joints with mechanical connections”, Buildings, 14(5), p. 1199. https://do 10.3390/buildings14051199.